Chemical Science

ARTICLE

Mechanical energy storage performances of The Aluminum Fumarate Metal–Organic Framework A520

Received 00th January 20xx,
Accepted 00th January 20xx

DOI: 10.1039/x0xx00000x

www.rsc.org/

Pascal. G. Yot,[*a] Louis Vanduyfhuis,[b] Elsa Alvarez,[c] Julien Rodriguez,[d] Jean-Paul Itié,[e] Paul Fabry,[c] Nathalie Guillou,[c] Thomas Devic,[c] Philip L. Llewellyn,[d] Veronique Van Speybroeck,[b] Christian Serre,[c] Guillaume Maurin,[a]

The aluminum Fumarate MOF A520 is revealed as a promising material for mechanical energy-related application with performances in terms of work and heat energies which surpass that of any porous solids reported so far. Complementary experimental and computational tools are deployed to finely characterize and understand the pressure-induced structural transition at the origin of this unprecedented level of performances.

1. Introduction

The family of crystalline hybrid porous solids known as metal organic frameworks (MOFs) has aroused a great interest over the past decade not only for the wide spectrum of materials that can be synthesized but also for their potential use in societally-relevant applications [MOF]. While much effort has been devoted to design MOF for gas storage/separation applications [MOF], much less attention has been paid to tune their mechanical energy storage performances [BEU11, SER12, YOT12, BERN13, GAS14, YOT14, ROD15, GRO15]. Only a few hydrophobic MOFs have been reported to absorb relatively high energy during water intrusion-exclusion cycles [ORT13, GRO15]. Alternatively, a series of flexible MOFs have been proposed as potential nano-dampers or shock absorbers since their pressure-induced structural transitions towards a contracted phase can generate relatively high work energy during compression/decompression cycles [BEU11, SER12, YOT12, BERN13, GAS14, YOT14, ROD15]. In particular, Hg-porosimetry and high-pressure X-ray diffraction experiments revealed that the carboxylate-based MIL-53 series rival or even surpass the mesoporous silica and zeolites in terms of mechanical energy stored. [ERO01, GRO13, ORT13, SAA10, KHA13] Very recently, some of us have significantly improved the crystallinity of the commercialized Aluminum fumarate A520 [ALV15+BASF] via an optimized synthesis route which rendered possible the resolution of the crystal structure of this solid in its hydrated form. This solid denoted as MIL-53(Al)-FA was revealed to be isostructural to MIL-53(Al)-BDC (BDC=1,4-benzenedicarboxylate) with a slightly smaller pore dimension (7.3 x 7.7 Å^2 vs 8.5 x8.5 Å^2) and interestingly a rigid character upon adsorption. Both features make this solid attractive to maximize the work energy (W = P×ΔV) absorbed during one compression-decompression cycle by an expected up-shifting of the structural transition pressure (P) due to the rigidity of its framework while maintaining a relatively high volume variation (ΔV) [MOF].

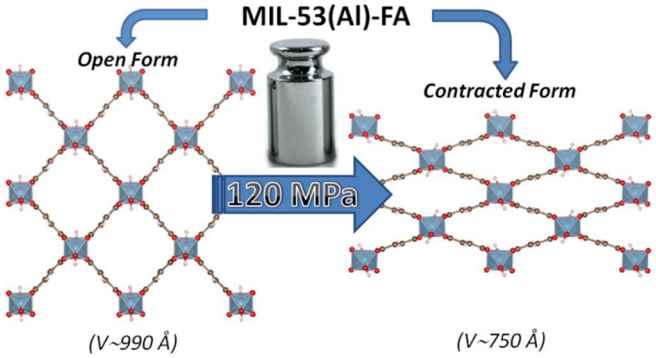

Fig. 1 *Schematic representation of the pressure-induced contraction of MIL-53(Al)-FA between an open and a contracted form.*

Hg-porosimetry and high-pressure X-ray powder diffraction coupled with molecular simulations confirmed that the dehydrated version of MIL-53(Al)-FA shows a structural contraction under an applied pressure above 100 MPa. This

[a] *Institut Charles Gerhardt Montpellier UMR 5253 CNRS UM ENSCM, Université de Montpellier, CC 15005, Place Eugène Bataillon, F-34095 Montpellier cedex 05, France. e-mail: pascal.yot@umontpellier.fr; Tel.: +33 4 67 14 32 94; Fax: +33 4 67 14 42 90.*
[b] *Centre for Molecular Modeling, Ghent University, Technologiepark 903, B-9052 Zwijnaarde, Belgium. Centre for Molecular Modeling, Ghent University, Technologiepark 903, B-9052 Zwijnaarde, Belgium.*
[c] *Institut Lavoisier Versailles, Université de Versailles St-Quentin, 45, avenue des Etats-Unis, F-78035 Versailles cedex, France.*
[d] *MADIREL, Aix-Marseille University, Centre Scientifique de St. Jérôme, F-13397 Marseille cedex 20, France.*
[e] *Synchrotron Soleil, L'orme des Merisiers, Saint-Aubin - BP 48, F-91192 Gif-sur-Yvette cedex, France.*
Electronic Supplementary Information (ESI) available: Experimental procedures, X-ray diffraction, and molecular simulation. See DOI: 10.1039/x0xx00000x

leads to a very high work energy of 60 J/g that considerably exceeds the values reported so far for other porous solids [BEU11, SER12, YOT12, BERN13, GAS14, YOT14, ROD15, GRO15,ERO01]. This unprecedented level of performances was maintained with the use of silicon oil, a more environmental friendly fluid, to perform the compression-decompression cycles. A direct measurement of the heat energy confirmed the great promises of this low-cost and stable MOF for such an application.

2. Material and methods

Powder of Aluminum Fumarate Metal–Organic Framework A520 has been prepared following the optimized synthesis route very recently devised by Alvarez *et al*. [ALV15]. The pressure-induced structure response of both hydrated and hydrated solids was characterized by mercury intrusion experiments [BEU10, YOT12, YOT14] using a mercury porosimeter Micromeritics Autopore 9240. Two intrusion-extrusion (compression-decompression) cycles were applied on the samples in the pressure range 10^{-4}-420 MPa (see ESI). Angle-dispersive X-ray powder diffraction (XRPD) data at high pressure (up to 1.88 GPa) was performed in-house using filtered Mo-Kα (λ=0.710730 Å) and at PSICHE beamline of the Synchrotron Soleil (Saint-Aubin, France) using a monochromatic beam (50×50 µm²) with the wavelength of λ=0.37380 Å. The pressure was generated with a membrane diamond anvil cell (MDAC) using silicon oil AP 100 (Aldrich) as pressure-transmitting medium as its kinetic diameter largely exceeds the window size of the fumarate which ensures that it does not enter inside the pores. The applied pressure was determined from the shift of the ruby R1 fluorescence line [MAO86]. The heat related to the pressure-induced structural transition of the dehydrated solid was determined using specifically devised calorimetry systems [ROD15] using silicon oil as pressure-transmitting medium.

Molecular simulations were performed to provide a structure model of the contracted phase detected under applied pressure. This computational effort was based on a newly *ab initio* derived flexible force-field for the MOF framework using the QuickFF protocol [VAN15]. All the details about experiments and modelling are available in ESI.

3. Results and discussion

The mechanical behavior of the hydrated MIL-53(Al)-FA was first explored by mercury intrusion and angle dispersive XRPD. Figure S1 reports the evolution of the cumulative volume of intruded mercury as a function of the applied pressure after two intrusion–extrusion (compression–decompression) cycles. Apart from the increase of the volume of Hg intruded below 10 MPa assigned to the compaction of the powder and the filling of the interparticular porosity, this curve does not show any step at higher pressure up to 420 MPa. This observation emphasizes that the hydrated solid does not undergo any structural change in this range of pressure. This holds also true at higher pressure as evidenced by high pressure XRPD experiments with the resulting XRPD patterns remaining unchanged up to 1.88 GPa (Figure S2). Referring to our previous computational investigation on the guest-modulation of the mechanical properties of MIL-53(Cr) [MA14], the absence of a structural phase transition is not necessarily due to the intrinsic robustness of the MOF framework but rather to the internal stress exerted by the water molecules which tends to put up resistance to the external applied pressure. To confirm this, the solid was further investigated in its dehydrated form. A structure model was first constructed starting with the crystal structure of the hydrated form and subsequently optimized by Density Functional Theory (DFT) calculations in the absence of the free water molecules (see ESI). This led to a structure with the same monoclinic $P2_1/c$ (No. 14) symmetry and a unit cell volume of 985 Å³ in good agreement with the experimental value (998.0(1) Å³) obtained from a pattern indexing (see Figure S3). Mercury porosimetry experiments performed on this solid (Figure 2) revealed a progressive increase of Hg intruded between 110 MPa and 400 MPa assigned to a contraction of the structure since Hg cannot penetrate inside micropores.

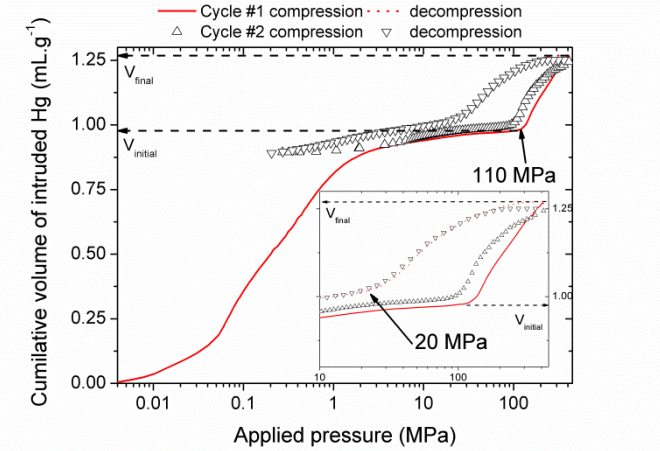

Fig. 2 *Cumulative volume of intruded mercury in two intrusion-extrusion cycles as a function of the applied pressure obtained for the MIL-53(Al)-FA sample ($V_{initial}$ and V_{final} are the volumes of mercury intruded before and after the contraction of the solid respectively).*

High pressure XRPD experiments further confirmed a structural change in the same range of pressure with the appearance of new Bragg peaks above 410 MPa (Figure 3). Although the XRPD resolution was not of sufficient quality to allow an indexation of the unit cell parameters, it was however possible to estimate the unit cell volume of the contracted phase using the Hg-porosimetry data. The increase in volume of mercury during the compression step is 0.25 mL.g^{-1}. Considering a unit cell volume of 998 Å³ for the pristine dehydrated structure, this leads to a contracted structure with a unit cell volume of ~750 Å³ which is significantly smaller than the cell dimensions of the pressure-induced phases previously observed for MIL-53(Al)-BDC (820 Å³) [YOT14], MIL-53(Cr)-BDC (931 Å³) [GHO12] and its MIL-47(V) (950 Å³) [YOT12] analogue. This highly degree of

contraction is rendered possible by the absence of the strong π-π interactions between the phenyl rings in the carboxylate-based MOFs which contribute to resist towards a more pronounced closure of the system.

A computational effort has been further deployed to propose a structure model for this contracted phase. Based on a newly *ab initio* flexible force-field derived for the MOF framework (see ESI), the energy profile of the MIL-53(Al)-FA structure as a function of its unit cell volume was calculated at 0 K (Figure S6). The optimized geometry at a fixed volume of 750 Å^3 encountered during this energy scan was proposed as a plausible structure model for this contracted phase. The reliability of this model was delivered by a relatively good accordance between the theoretical XRPD pattern calculated for this predicted structure and the corresponding experimental data collected at 410 MPa (Figure S7). In a similar way than for the MIL-53-BDC analogues, the structural shrinkage leads to a significant decrease of the Al-Oc-Cc-Cg2 dihedral angle from 180° (pristine phase) to 155° (contracted phase). This emphasizes that the rotation of the linker about the Oc-Oc axis is also the driving force for the structural transition of MIL-53(Al)-FA [YOT12, YOT14].

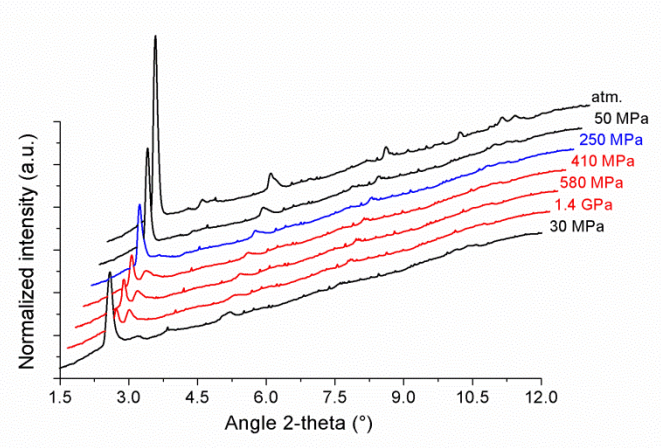

Fig. 3 *X-ray powder diffraction patterns of the MIL-53(Al)-FA as a function of the applied pressure (λ=0.37380 Å). Patterns in black correspond to the open form, in blue mixture of open and contracted form and in red contracted form.*

The compression step occurs at a pressure which is significantly higher than that observed either for MIL-53(Al)-BDC (55 MPa), MIL-53(Cr)-BDC (55 MPa), or MIL-47(V)-BDC (85 MPa). This implies that the work energy stored by MIL-53(Al)-FA that can be calculated from the pressure transition and the corresponding volume variation, attains 60 J.g^{-1}. This value largely exceeds the performances of all the porous solids reported so far by at least a factor 5 (see Table 1).

Table 1 *Comparison of the work energy performance of MIL-53(Al)-FA, with that of other porous solids.*

	Work (J.g^{-1})	$P_{transition}$ (MPa)	Reference
MIL-53(Al)-FA	60	110	This work
MIL-53(Al)-BDC	7	18	[YOT14]
MIL-53(Cr)-BDC	16	55	[BEU11]
MIL-47(V)-BDC	33	125	[YOT12]
ZIF-8	13.3		[ORT13]
Silicalite	11		[TZA14]
ITQ-4, ITQ-12 zeolites	5.7-8.1		[KHA14, SAA10]
SBA-15 mesoporous silica	4.3-6.1		[GOK13]

Mercury intrusion further evidenced that MIL-53(Al)-FA shows a fully reversible mechanical behavior upon compression-decompression cycles with the presence of a hysteresis of about 125 MPa. This was confirmed by high pressure XRPD which revealed that the contracted version of MIL-53(Al)-FA returns to the initial form once the pressure is released (Figure 3). These observations make this solid as a promising candidate for mechanical energy storage application and particularly in the form of nano-dampers. However for application purposes, mercury cannot be considered as pressure transmitting medium due to very high toxicity. We envisaged as a further step the use of a more friendly environmental fluid, the silicon oil to perform cycles of compression/decompression on MIL-53(Al)-FA (see ESI). The corresponding data are reported in Figure 4.

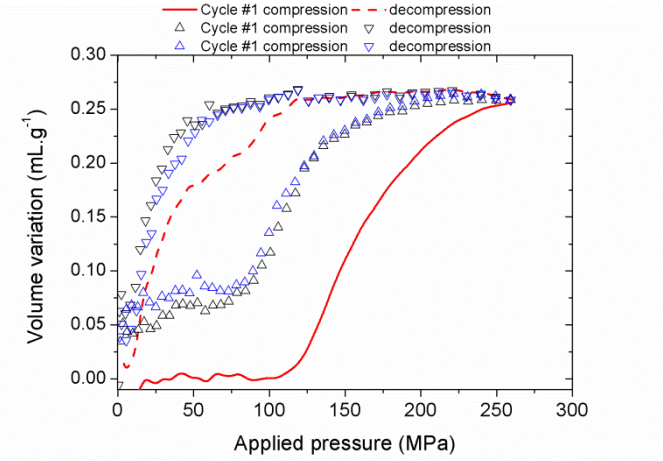

Fig. 4 *Unit cell volume variation of MIL-53(Al)-FA as a function of the applied oil pressure during three compression-decompression cycles.*

In contrast with the Hg experiment, the increase of the volume at low pressure is not present anymore as the silicone oil is a wetting fluid that can spontaneously occupy the interparticular porosity domain. A step for cycle 1 occurs in the pressure range [100-250 MPa] and leads to a volume variation of 0.25 mL/g^{-1}. Both observations concur very well with the values obtained with mercury porosimetry, the lower upper pressure vs Hg being associated with the limit of the current oil system (250 MPa) compared to the mercury set-up (400 MPa). This strongly supports that the selected silicon oil is enough bulky to do not penetrate into the MOF micropores and hence this fluid can be

used to allow the monitoring of the pressure-induced structural transition of MIL-53(Al)-FA.

The silicon oil compression-decompression cycle presents a hysteresis consistent with the Hg porosimetry and the work energy stored 41.7 J.g^{-1} remains very high. Both features confirm the promises of this solid as a potential nano-damper. A partial loss of volume and a decreasing of the transition pressure are recorded after the first compression (from 0.25 mL.g^{-1} and 100-250 MPa for the first cycle to 0.20 mL.g^{-1} and 72-250 MPa for other cycles respectively) which might be due to the interactions between the MOF surface and the silicon oil [ROD15]. However, the performances in terms of work energy stored remain very high (22.9 J.g^{-1}, see Table 2) and the cycles are superimposed, within experimental error.

The heat dissipated by the structural transition of the MIL-53(Al)-FA during the first compression/decompression cycle was further assessed by calorimetry measurements. The corresponding data are reported in Figure 5. It is shown that the compression (contraction of the structure) is exothermic while the decompression (expansion of the structure) is endothermic and this trend is consistent with that previously reported for MIL-53(Al)-BDC [ROD15]. Table S1 evidences that in terms of dissipated heat energy, MIL-53(Al)-FA also largely outperforms all the porous solids, i.e. other MOFs and hydrophobic silica. It is also shown that after the first cycle, the heating energy (i.e. difference in heat of compression and decompression energy) is around -18.7 J.g^{-1} which is significantly higher that the value obtained for MIL-53(Al)-BDC (-5 to -6 J.g^{-1} cycle 1 [ROD15]). This suggests that a heat evacuation protocol would need to be implemented for the use of this solid as nano-damper. Finally, Table 1 emphasizes that the work and heat energies are significantly different resulting in internal energy (U) (-8.4 to 6.9 J g^{-1}) much higher than the value previously reported for MIL-53(Al)-BDC (-3.0 to 1.0 J g^{-1}).

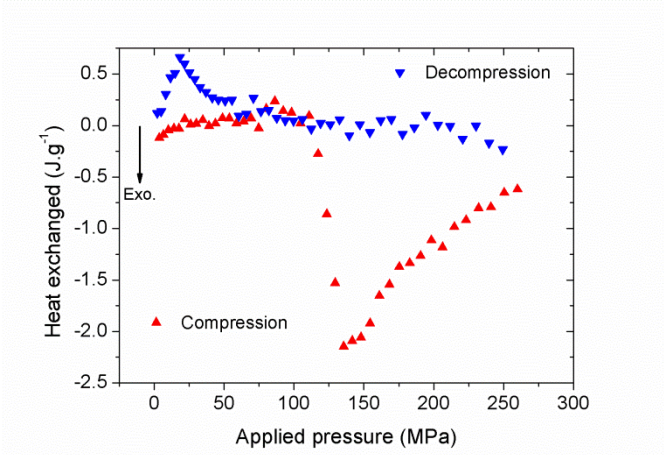

Fig. 5 *Heat energy obtained for MIL-53(Al)-FA as a function of the pressure during the first cycle release. Red Up-triangles correspond to compression and blue down-triangles decompression.*

Table 2 *Experimental energetic data of compression/decompression cycles on the MIL-53(Al)-FA.*

	Work (J.g^{-1})	Heat (J.g^{-1})	Internal energy (J.g^{-1})
Cycle 1: Compression	41.7	-25.1	16.6
Cycle 1: Decompression	-10.8	6.4	-4.4
Cycle 2: Compression	22.9	-18.7	4.2
Cycle 2: Decompression	-8.0	6.3	-1.7
Cycle 3: Compression	22.2	-18.2	4.0
Cycle 3: Decompression	-8.8	6.5	-2.3

Conclusions

The family of flexible MOFs is a great source of potential candidates for mechanical-energy related applications by virtue of their reversible/irreversible structural switching towards a more contracted phase that can be provoked by the application of a high external pressure. Amongst them, the Aluminum fumarate A520 represents the best porous solid reported so far with outstanding performances in terms of work and heat energies. This commercialized material is particularly attractive since its low-production cost, low toxicity and high stability will be not a drawback for further device development following the concept of MOF/silicon oil system proposed in this study.

Acknowledgements

The authors would like to thank the French National Agency for Research ANR "MODS" (ANR-12-BS10-0005) for its financial supports. Dr. J. Haines (ICGM) is also thanked for the its support for X-ray diffraction on hydrated form of MIL-53(Al)-FA. We acknowledge the French national synchrotron radiation source "Synchrotron Soleil" (Saint-Aubin, France) and PSICHE beamline for beam time. G.M. thanks Institut Universitaire de France for its support.

Notes and references

[ALV15]E. Alvarez, N. Guillou, C. Martineau, B. Bueken, B. Van de Voorde, C. Le Guillouzer, P. Fabry, F. Nouar, F. Taulelle, D. de Vos, J.-S. Chang, K. Ho Cho, N. Ramsahye, T. Devic, M. Daturi, G. Maurin, C. Serre, *Angew. Chem. Int. Ed.*, 2015, **54**, 3664-3668.

[BEN13]7 T. D. Bennett, P. J. Saines, D. A. Keen, J. C. Tan and A. K. Cheetham, Chem. – Eur. J., 2013, **19**, 7049.

[BEU10]I. Beurroies, M. Boulhout, P. L. Llewellyn, B. Kuchta, G. Férey, C. Serre, R. Denoyel, *Angew. Chem., Int. Ed.*, 2010, **49**, 7526.

[DO03]M. B. Dogruoz, E. L. Wang, F. Gordaninejad, A. J. Stipanovic, J. *of Intel. Mater. Syst. and Struc.*, 2003, **14**, 79.

[ELS99]P. S. Els, B. Grobbelaar, *J. of Terramechanics*, 1999, **36**, 197.

[ERO01]V. Eroshenko, R. C. Regis, M. Soulard and J. Patarin, *J. Am. Chem. Soc.*, 2001, **123**, 8129.

[FER08]G. Férey, Chem. *Soc. Rev.*, 2008, **37**, 191.

[GAA12]M. Gaab, N. Trukhan, S. Maurer, R. Gummaraju, U. Mueller, Microporous Mesoporous Mater. 2012, **157**, 131.

[GAS14]J. Gascon, A. Corma, F. Kapteijn and F. Llabre´s i Xamena, ACS Catal., 2014, **4**, 361.

[GHO12]A. Ghoufi, A. Subercaze, Q. Ma, P. G. Yot, Y. Ke, I. Puente Orench, T. Devic, V. Guillerm, C. Zhong, C. Serre, G. Férey and G. Maurin, *J. Phys. Chem. C*, 2012, **116**, 13289.
[GOK13] N. Gokulakrishnan, J. Parmentier, M. Trzpit, L. Vonna, J.L. Paillaud, M. Soulard, *J Nanosci Nanotechno* **2013**, *13*, 2847.
[GRO15]Y. Grosu, G. Renaudin, V. Eroshenko, J.-M. Nedelec, J.-P. E. Grolier, *Nanoscale*, 2015, **7**, 8803.
[KHA13] I. Khay, L. Tzanis, T. J. Daou, H. Nouali, A. Ryzhikov, J. Patarin,Phys. Chem. Chem. Phys. 2013, 15, 20320.
[LEU10]a) E. Leung, U. Mller, G. Cox, H. Mattenheimer, S. Blei, EP Patentanmeldung 10183283.0, 2010; b) F. Jeremias, D. Frçhlich, C. Janiak, S. K. Henninger, RSC Adv. 2014, 4, 24073.
[MA14]Q. Ma, Q. Yang, A. Ghoufi, M. Lei, G. Férey, C. Zhong, G. Maurin, J. Mater. Chem. A, 2014, **2**, 99691.
[MOF]Themed issues: metal-organic frameworks, a) *Chem. Rev.* 2012, **112**, 673; b) *Chem. Soc.* Rev. 2014, **43**, 5415.
[MUE04] U. Mueller, G. Luinstra, O. M. Yaghi, US Pat. 6 617 467, 2004, BASF Aktiengesellschaft.
[OR15] G. Ortiz, H. Nouali, C. Marichal, G. Chaplais, J. Patarin, Phys.Chem. Chem. Phys. 2013, 15, 4888
[SAA10] M. A. Saada, S. Rigolet, J.-L. Paillaud, N. Bats, M. Soulard, J. Patarin, J. Phys. Chem. C 2010, 114, 11650.
[SER12] P. Serra-Crespo, E. Stavitski, F. Kapteijn and J. Gascon, RSC Adv.,2012, **2**, 5051.
[TZA14] L. Tzanis, H. Nouali, T. J. Daou, M. Soulard, J. Patarin, Mater. Lett. 2014, 115, 229–232.
[VAN15]L. Vanduyfhuys, S. Vandenbrande, T. Verstraelen, R. Schmid, M. Waroquier, V. Van Speybroeck. *J. Comput. Chem.* 2015, **36**, 1015.
[YOT12]P.G. Yot, Q. Ma, J. Haines, Q. Yang, A. Ghoufi, T. Devic, C. Serre, V. Dmitriev, G. Férey, C. Zhong, G. Maurin, *Chem. Sci.*, 2012, **3**, 1100.
[YOT14]P. G. Yot, Z. Boudene, J. Macia, D. Granier, L. Vanduyfhuys, T. Verstraelen, V. Van Speybroeck, T. Devic C. Serre, G. Férey, N. Stock, G. Maurin, *Chem. Comm.*, 2014, **50**, 9462.

1 Citations should appear here in the format A. Name, B. Name and C. Name, *Journal Title*, 2000, **35**, 3523; A. Name, B. Name and C. Name, *Journal Title*, 2000, **35**, 3523.
2 …